INL/CON-06-11716
PREPRINT

Thermal and Electrochemical Performance of a High-Temperature Steam Electrolysis Stack

2006 Fuel Cell Seminar

J. O'Brien
C. Stoots
J. Herring
G. Hawkes
J. Hartvigsen

November 2006

The INL is a
U.S. Department of Energy
National Laboratory
operated by
Battelle Energy Alliance

Thermal and Electrochemical Performance of a High-Temperature Steam Electrolysis Stack

J. O'Brien[1], C. Stoots[1], J. Herring[1], G. Hawkes[1], J. Hartvigsen[2]
[1]Idaho National Laboratory, Idaho Falls, ID
[2]Ceramatec, Inc., Salt Lake City, UT

INTRODUCTION

Currently there is strong interest in the large-scale production of hydrogen from non-fossil sources. This interest is driven by the immediate demand for hydrogen for refining of increasingly low-quality petroleum resources, the expected intermediate-term demand for carbon-neutral synthetic fuels, and the possible long-term demand for hydrogen as an environmentally benign transportation fuel [1, 2]. Currently hydrogen is produced primarily via steam reforming of methane. From a long-term perspective, alternatives to methane reforming are sought for large-scale production of hydrogen as a major energy carrier since such fossil fuel conversion processes consume non-renewable resources and emit greenhouse gases to the environment. Consequently, production of hydrogen from water splitting via either electrolytic or thermochemical processes is under consideration. The hydrogen production efficiency of any thermal water-splitting process increases with temperature, so high-temperature operation is desirable.

Development of advanced high-temperature nuclear reactors could enable high-efficiency large-scale hydrogen production, with no consumption of fossil fuels, no production of greenhouse gases, and no other forms of air pollution. High-temperature electrolytic water-splitting supported by nuclear process heat and electricity has the potential to produce hydrogen with high overall system efficiencies similar to those of the thermochemical processes, but without the corrosive conditions of thermochemical processes and without the fossil fuel consumption and greenhouse gas emissions associated with hydrocarbon processes. Specifically, a high-temperature advanced nuclear reactor coupled with a high-efficiency power cycle and a high-temperature electrolyzer could achieve competitive thermal-to-hydrogen conversion efficiencies of 45 to 55% at 850°C.

A research program is under way at the Idaho National Laboratory (INL) to simultaneously address the research and scale-up issues associated with the implementation of solid-oxide electrolysis cell technology for hydrogen production from steam. We are conducting a progression of electrolysis stack testing activities, at increasing scales, along with a continuation of supporting research activities in the areas of materials development, single-cell testing, detailed computational fluid dynamics (CFD) and systems modeling. This paper will present recent experimental results obtained from testing of planar solid-oxide stacks operating in the electrolysis mode. The hydrogen-production and electrochemical performance of these stacks will be presented, over a range of operating conditions. In addition, internal stack temperature measurements will be presented, with comparisons to computational fluid dynamic predictions.

EXPERIMENTAL APPARATUS

A schematic of the electrolysis stack-testing apparatus is presented in Fig. 1. Inlet gas flow rates of nitrogen, hydrogen and air are established and maintained by means of precision mass-flow controllers. Nitrogen is used as an inert carrier gas. Hydrogen is included in the inlet flow (5-10% by volume) as a reducing gas in order to help prevent oxidation of the Nickel cermet electrode material. The nitrogen / hydrogen gas mixture is mixed with steam by means of a humidifier. The dewpoint temperature of the nitrogen / hydrogen / steam gas mixture exiting the humidifier is monitored continuously using a precision dewpoint sensor. Another dewpoint sensor is located downstream of the electrolysis stack, providing an independent measurement of the steam consumption and corresponding hydrogen production rate. Since the vapor pressure of the water and the resulting partial pressure of the steam exiting the humidifier are determined by the water bath temperature, the water vapor mass flow rate is directly proportional to the carrier gas flow rate for a specified bath temperature. Also, since the nitrogen and hydrogen flow rates are fixed by the

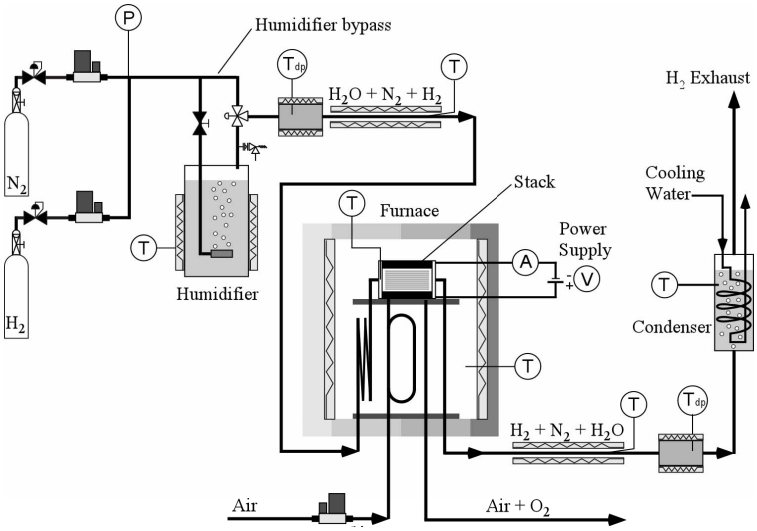

Figure 1. Schematic of experimental apparatus for electrolysis stack testing.

mass flow controllers, and the steam partial pressure is fixed by the bath temperature, the complete gas composition is precisely known at all times. All gas lines located downstream of the humidifier are heat-traced in order to prevent steam condensation. The humidifier also incorporates a pressure relief valve to avoid any possibility of over-pressurization. Additional details of the experimental apparatus and data reduction are presented in reference [3].

A close-up photograph of a 25-cell planar solid-oxide electrolysis stack used for electrolysis testing is shown in Fig. 2. The stack was fabricated by Ceramatec, Inc. of Salt Lake City, Utah. Per-cell active area is 64 cm^2. It is designed to operate in cross flow, with the steam/hydrogen gas mixture entering the inlet manifold on the right of Fig. 2, and exiting through the outlet manifold, visible on the left. Air flow enters at the rear though an air inlet manifold (not visible in Fig. 2) and exits at the front directly into the furnace. The power lead attachment tabs, integral with the upper and lower interconnect plates are also visible in Fig. 2. Additional instrumentation is also visible in Fig. 2(b), including 4 intermediate voltage taps and 5 miniature thermocouples inserted into the air flow channels to monitor internal stack temperatures. The thermocouples were inconel-sheathed 0.020-inch OD, mineral-insulated, type-K, ungrounded. Stack interconnect plates include an impermeable ferritic stainless steel separator plate (~0.46 mm thick) with edge rails and two corrugated "flow fields," one on the air side and one on the steam/hydrogen side. The height of the flow channel formed by the edge rails and flow fields is 1.0 mm. Each flow field includes 32 perforated flow channels across its width to provide uniform gas-flow distribution. The steam/ hydrogen flow field is fabricated from nickel foil. The air-side flow field is ferritic stainless steel. The interconnect plates and flow fields also serve as electrical conductors and current distributors.

The cells are electrolyte-supported, with scandia-stabilized zirconia electrolytes, about 140 μm thick. Scandia-stabilized zirconia electrolytes exhibit significantly higher ionic conductivity compared to the more common yttria-stabilized zirconia. The air-side electrode, is a strontium-doped manganite. The electrode is graded, with an inner layer of manganite/zirconia (~13 μm) immediately adjacent to the electrolyte, a middle layer of pure manganite (~18 μm), and an outer bond layer of cobaltite. The steam/ hydrogen electrode is also graded, with a nickel-zirconia cermet layer (~13 μm) immediately adjacent to the electrolyte and a pure nickel outer layer (~10 μm).

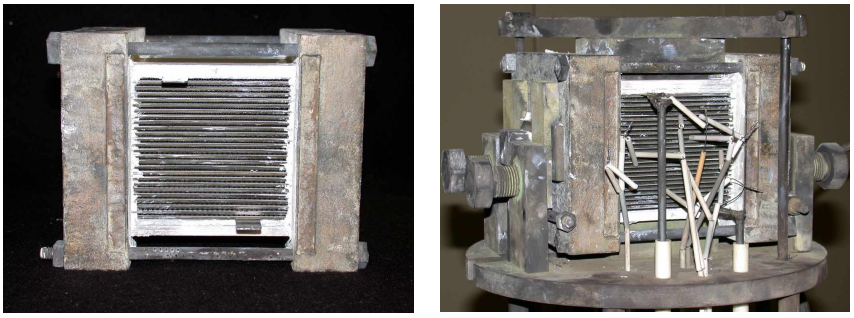

(a) (b)

Figure 2. 25-cell planar stack; (a) front view of stack prior to installation, (b) instrumented stack on test stand.

Two types of stack characterization tests were performed: DC potential sweeps and long-term tests. DC potential sweeps were performed by varying the applied stack voltage over a range, typically from 0.8 V to 1.8 V/cell. Applied voltage values lower (in magnitude) than the open-cell potential (~ 0.9 V/cell) yield the fuel-cell mode of operation while applied voltages higher than the open-cell value yield electrolysis. Results of the DC potential sweeps allow for determination of the stack area-specific resistance (ASR) and hydrogen production rates over a range of conditions. Long-term tests were performed by selecting an appropriate stack operating voltage and observing the hydrogen-production performance over a relatively long period of time, to determine long-term degradation characteristics.

RESULTS

Results of several representative sweeps are shown in Fig. 3(a) in the form of polarization curves, representing per-cell operating voltage versus current density. Test conditions for each of the seven sweeps are tabulated in the figure. Five of the sweeps were obtained from a 10-cell stack (sweeps 10-1 through 10-5) and two were obtained from a 25-cell stack (25-1 and 25-2). Theoretical open-cell potential values are shown in the figure for each sweep using a single data point at zero current density. Note that the measured open-cell potentials are in excellent agreement with the theoretical values for each sweep. Sweep 10-1 was performed with a relatively low inlet steam flow rate, corresponding to the low inlet dewpoint value of 48.5ºC and relatively low nitrogen and hydrogen flow rates. This sweep has a relatively high slope on i-V coordinates, indicating a relatively high ASR. This sweep also clearly shows the effects of steam starvation; the slope of the *i-V* curve increases dramatically as the current density is increased. The outlet dewpoint temperature corresponding to the highest current density shown in this figure was only 4ºC for this sweep. Sweep 10-2 was performed at an intermediate steam concentration, with an inlet dewpoint temperature of 70ºC. This sweep exhibits nearly linear behavior over the range of current densities shown, with a much smaller slope than sweep 10-1. Sweeps 10-3 and 10-4 are nearly linear at low current densities, then slightly concave-down at higher current densities. Sweep 10-5 has a shallower slope than the others, consistent with the higher operating temperature of 830ºC. Sweep 25-1 was performed in a stepwise fashion, rather than as a continuous sweep. This was done in order to ensure sufficient time for the internal stack temperatures to achieve steady-state values at each operating voltage. Note that the slope of this sweep is small, indicating low *ASR* (~1.5 $\Omega \cdot cm^2$). This sweep was performed at the beginning of a 1000-hour long-duration 25-cell stack test. Sweep 25-2 was acquired at the end of the long-duration test. The stack operating temperature was increased form 800°C to 830°C part way through the test. Note that the slope of sweep 25-2 is higher than that of sweep 25-1, despite the higher temperature, due to performance degradation over 1000 hours of operation.

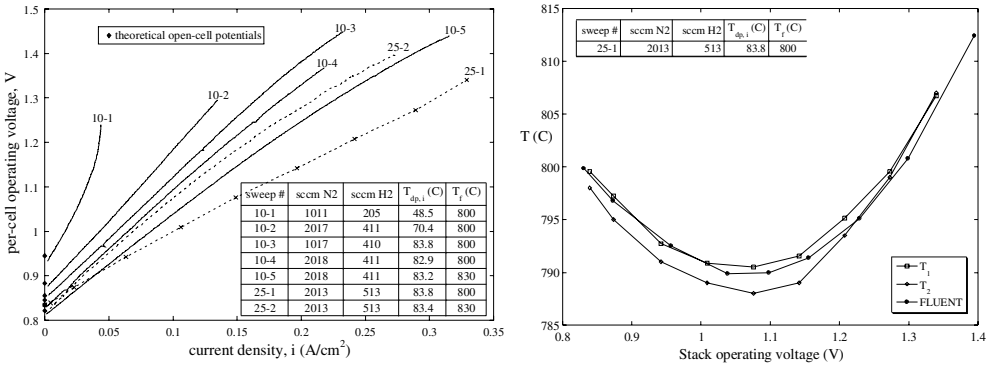

Figure 3. (a) Stack temperatures measured during DC potential sweep; (b) Stack operating potentials as a function of current density, 10-cell stack and 25-cell stack.

Internal stack temperatures measured during a DC potential sweep are presented in Fig. 3(b) as a function of operating voltage at a furnace temperature of 800°C. These temperature measurements were obtained using miniature thermocouples inserted to a depth of 5 cm into the air flow channels of the 25-cell stack. Stack internal thermocouple T_1 was located in the center air flow channel, halfway between the midpoint and the steam/hydrogen inlet. Stack internal thermocouple T_2 was inserted into the center position of the fifth cell from the bottom of the stack. The internal stack thermocouples respond as expected during the sweep. At voltages between the open-cell potential and the thermal neutral voltage, in the electrolysis mode, the stack internal temperatures are lower than the gas inlet and furnace setpoint temperatures because at this operating voltage, the endothermic reaction heat requirement is greater than the ohmic heating and there is a net cooling effect on the stack. A thermal minimum point is reached at an operating voltage that is halfway between the open-cell voltage and the thermal-neutral voltage (~1.06 V in Fig. 3(b)) and full thermal recovery is observed near the thermal neutral voltage of 1.29 V. The magnitude of the stack cooling and heating effects is greatest at the center of the stack. We have predicted similar internal stack temperature trends using a three-dimensional CFD model of a planar electrolysis cell. The model replicates the geometry of a single cell as it exists in a stack. It was created using *FLUENT* with an SOFC user-defined subroutine, operating in the electrolysis mode. Mean electrolyte temperatures predicted from our *FLUENT* CFD model under corresponding operating conditions are also presented in Fig. 3(b). The CFD model includes a radiant boundary condition around the periphery of the cell to simulate the furnace environment. The agreement between the measured internal stack temperatures and the CFD model predictions is excellent.

CONCLUSIONS

High-temperature steam electrolysis appears to be a viable technology for high-efficiency hydrogen production. Future research will address improvements in cell performance and long-term degradation.

References

1. FORSBERG, C. W., "The Hydrogen Economy is Coming. The Question is Where?" *Chemical Engineering Progress*, December, 2005, pp. 20-22.
2. National Academy of Sciences, National Research Council, *The Hydrogen Economy: Opportunities, Costs, Barriers, and R&D Needs*, February, 2004.
3. O'Brien, J. E., Stoots, C. M., Herring, J. S., and Hartvigsen, J. J.,"Hydrogen Production Performance of a 10-Cell Planar Solid-Oxide Electrolysis Stack," *Journal of Fuel Cell Science and Technology*, Vol. 3, pp. 213-219, May, 2006.